Supplemental information includes Supplemental Data (seven Supplemental Figures and two Supplemental Tables), Extended Experimental Procedures and Supplemental References.

Supplemental Data

Figure S1 (sung)

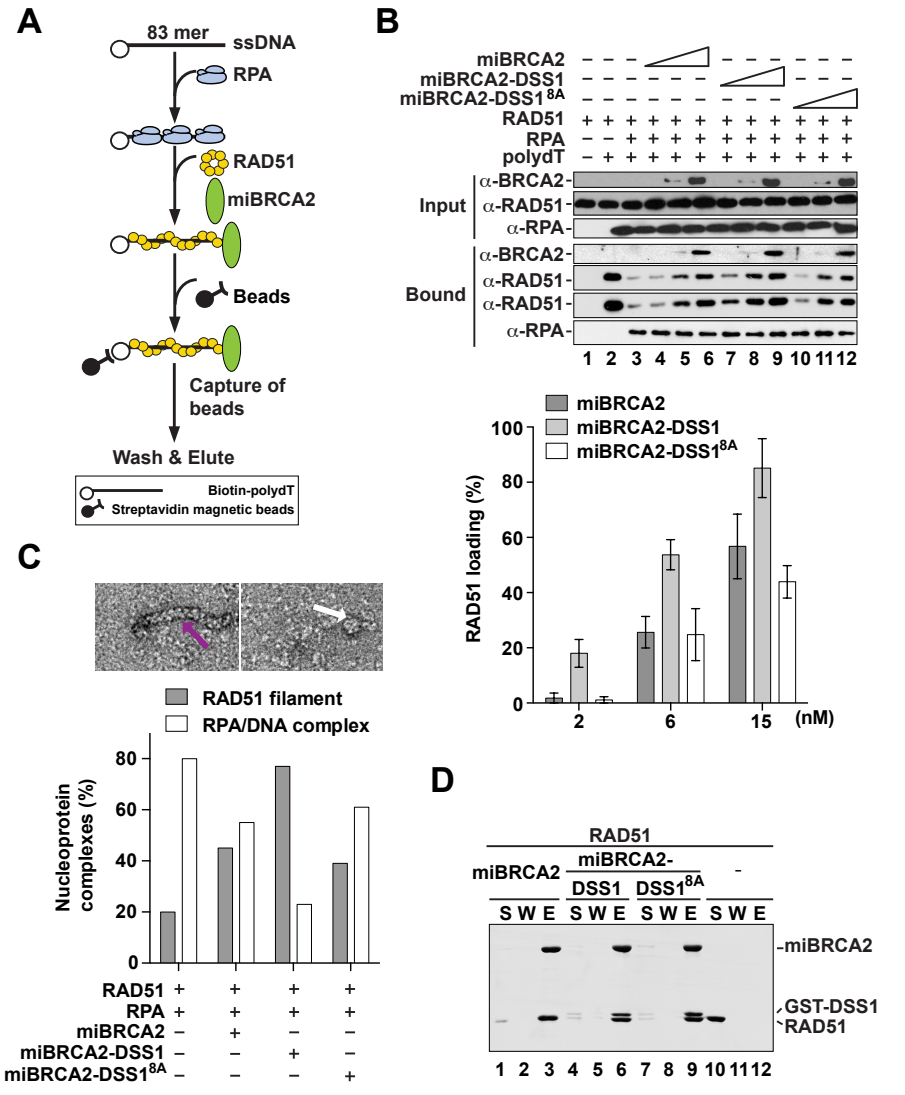

Figure S1. Role of DSS1 in miBRCA2-dependent RAD51 presynaptic filament assembly, related to Figure 1 and Figure 4.

(A) Schematic of the magnetic bead-based pulldown assay to test for RAD51 loading onto RPA-coated dT_{83}.

(B) Western blot analyses to monitor RAD51 loading by miBRCA2, miBRCA2-DSS1 or miBRCA2-DSS1^{8A} onto the DNA substrate. The mean values (± s.d.) from three independent experiments were plotted.

(C) EM analysis of miBRCA2, miBRCA2-DSS1 or miBRCA2-DSS1^{8A} to enhance RAD51 presynaptic filament assembly. The proportions of RPA-ssDNA complex (white arrow) and RAD51-ssDNA nucleoprotein filament (purple arrow) were determined for the four reactions (995, 993, 959 and 924 nucleoprotein complexes were counted, respectively).

(D) Pulldown assay to test for interaction of RAD51 with either miBRCA2, miBRCA2-DSS1 or miBRCA2-DSS1^{8A} via the $(His)_6$ tag on miBRCA2. The supernatant (S) containing unbound proteins, the wash (W), and the eluate (E) fractions were analyzed.

Figure S2 (sung)

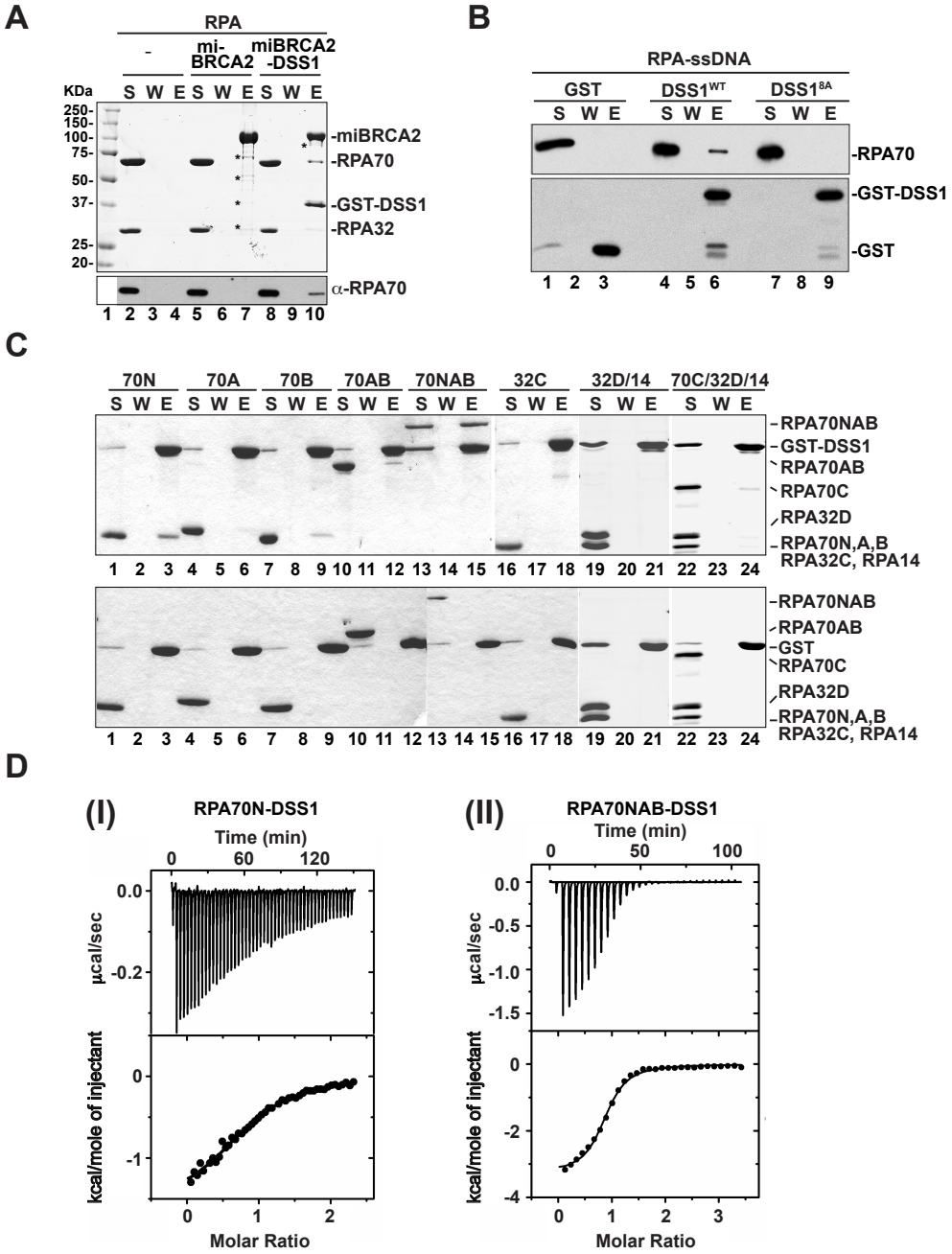

Figure S2. Characterization of DSS1 for its interaction with RPA fragments, related to Figure 2 and Figure 3.

(A) Pulldown assay to test for the interaction between RPA and miBRCA2 or miBRCA2-DSS1 via the $(His)_6$ tag on miBRCA2. The supernatant (S) containing unbound proteins, the wash (W), and the eluate (E) fractions were analyzed by SDS-PAGE and Coomassie Blue staining and by immunoblotting for RPA. The asterisks highlight minor proteolytic products and contaminants in the protein preparations.

(B) Pulldown assay to test for the interaction of the RPA-ssDNA complex with DSS1 via the GST tag on the latter. The supernatant (S) containing unbound proteins, the wash (W), and the eluate (E) fractions were analyzed by SDS-PAGE by immunoblotting for RPA and DSS1.

(C) Pulldown assay to test for the interaction between the indicated RPA fragments and DSS1 via the GST tag on the latter. GST alone was included as control. The supernatant (S) containing unbound proteins, the wash (W), and the eluate (E) fractions were analyzed.

(D) Isothermal titration calorimetry of the interaction of DSS1 with RPA70N (I) and RPA70NAB (II). The upper panel shows raw heat release upon addition of DSS1 onto solution containing either RPA70N or NAB. The lower panel shows the integrated raw injection points.

Figure S3 (sung)

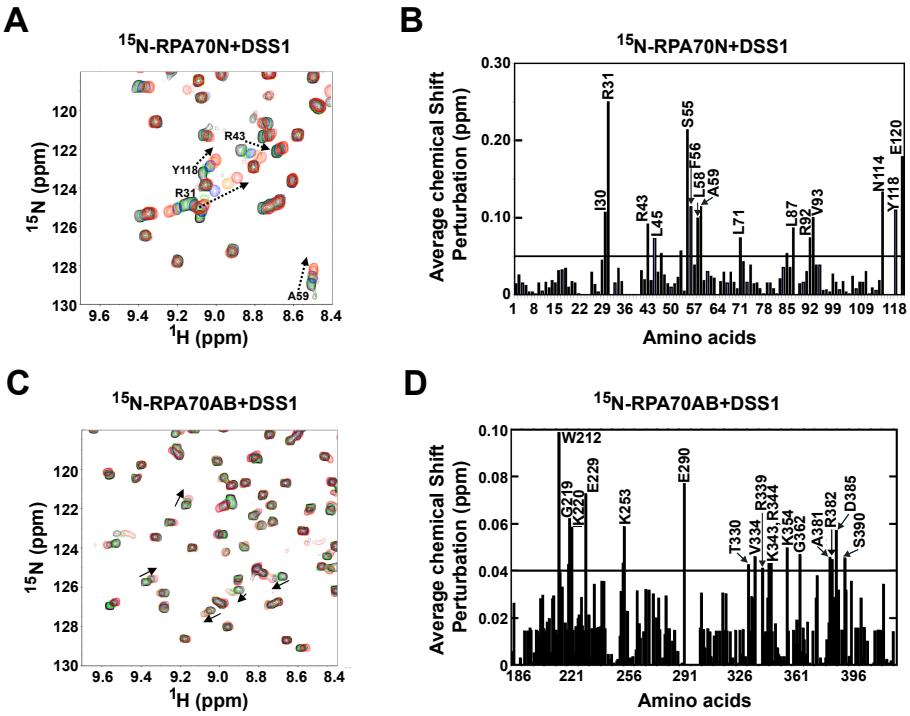

E

The chemical shift residues on RPA70N & AB subdomain structures

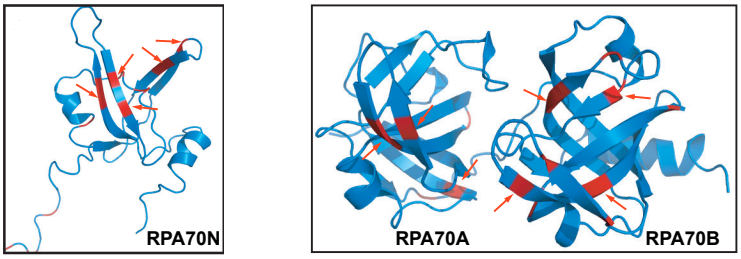

Figure S3. NMR analyses to define the interaction interfaces on DSS1 and RPA, related to Figure 3.

(A) Overlay of ^{15}N-HSQC spectra of ^{15}N-enriched RPA70N as the solution is titrated with DSS1.

(B) Chemical shift changes plotted against the sequence of RPA70N. The mean value of chemical shift changes is depicted by the solid horizontal line.

(C) Overlay of ^{15}N-HSQC spectra of ^{15}N-enriched RPA70AB upon titration with DSS1.

(D) Chemical shift changes plotted against the sequence of RPA70AB. The mean value of chemical shift changes is depicted by the solid horizontal line.

(E) Residues with a chemical shift greater than the mean value (colored red) depicted on the structure of RPA70N and AB with arrows using the data collected in binding experiments for individual RPA70N and RPA70AB.

Figure S4 (sung)

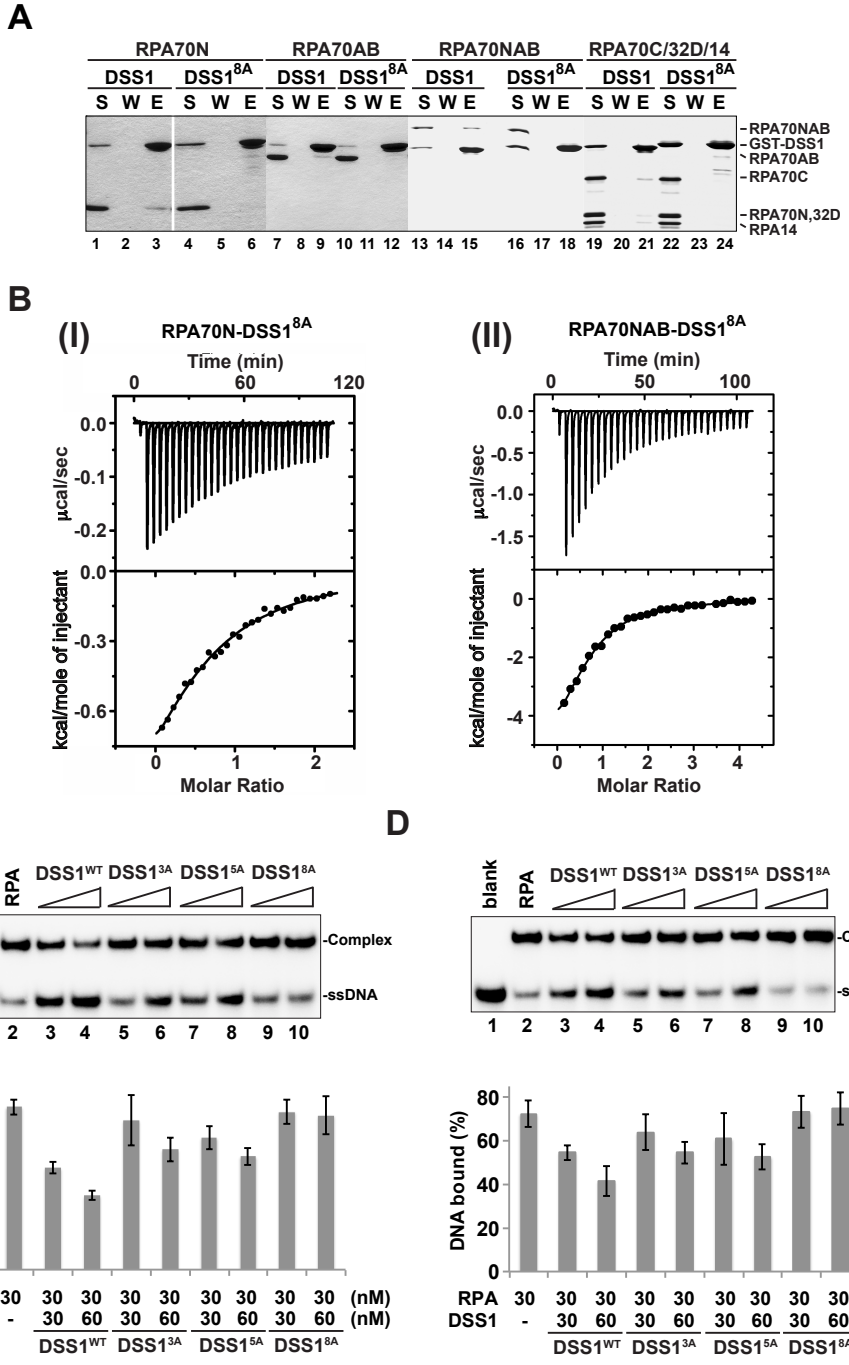

Figure S4 (sung)

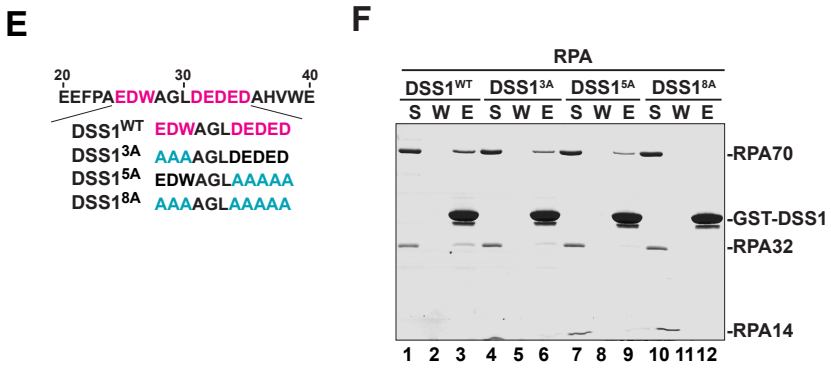

Figure S4. Characterization of DSS1 mutants for their interactions with RPA fragments and their ability to inhibit the DNA binding activity of RPA, related to Figure 2 and Figure 4.

(A) Pulldown assays to test the interaction between DSS1^{8A} and RPA70N, RPA70AB, RPA70NAB or RPA70C/32D/14 via the GST tag on DSS1. The supernatant (S) containing unbound proteins, the wash (W), and the eluate (E) fractions were analyzed.

(B) Isothermal titration calorimetry of the interaction of DSS1^{8A} with RPA70N (I) and RPA70NAB (II). The upper panel shows raw heat release upon addition of DSS1 onto solution containing either RPA70N or NAB. The lower panel shows the integrated raw injection points.

(C) The effect of DSS1, DSS1^{3A}, DSS1^{5A} and DSS1^{8A} on DNA binding by RPA was examined by co-incubating ssDNA with RPA and DSS1 or the indicated DSS1 mutant. The mean values (± s.d.) of data from three independent experiments were plotted.

(D) The effect of DSS1, DSS1^{3A}, DSS1^{5A} and DSS1^{8A} on DNA binding by RPA was examined by adding DSS1 or the indicated DSS1 mutant to the pre-formed RPA-

ssDNA complex. The mean values (± s.d.) of data from three independent experiments were plotted.

(E) The RPA interaction domain in DSS1 and the mutated residues in DSS1^{3A}, DSS1^{5A} and DSS1^{8A} mutants.

(F) Pulldown assay to test for the interaction of RPA with DSS1, DSS1^{3A}, DSS1^{5A} and DSS1^{8A} via the GST tag on the latters. The supernatant (S) containing unbound proteins, the wash (W), and the eluate (E) fractions were analyzed.

Figure S5 (sung)

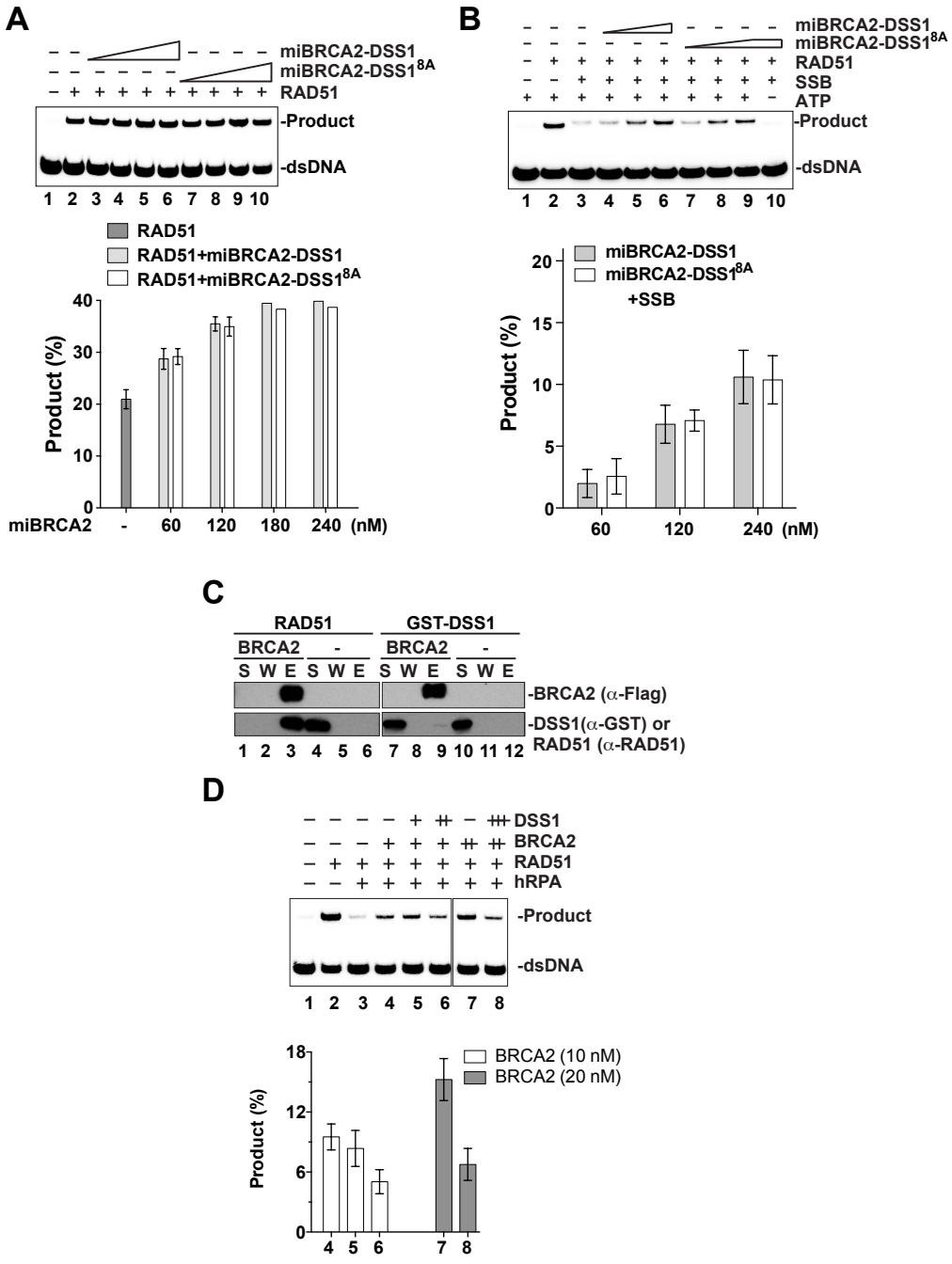

Figure S5. Characterization of miBRCA2-DSS1^{8A} for its recombination mediator activity and role of DSS1 in BRCA2/RAD51-mediated homologous DNA pairing and strand exchange, related to Figure 4 and Figure 5.

(A) miBRCA2-DSS1 and miBRCA2-DSS1^{8A} were tested for the ability to stimulate RAD51-mediated homologous DNA pairing without RPA in the reaction. The mean values (± s.d.) from three independent experiments were plotted.

(B) miBRCA2-DSS1 and miBRCA2-DSS1^{8A} complexes were tested for their mediator activity with SSB-coated ssDNA. The mean values (± s.d.) from three independent experiments were plotted.

(C) Pulldown assay to test for the interaction between DSS1 and full length BRCA2 via the MBP tag on the latter; RAD51 was included as positive control. BRCA2 (1 μg) was incubated with RAD51 (0.1 μg) or GST-DSS1 (0.1 μg). The supernatant (S) containing unbound proteins, the wash (W), and the eluate (E) fractions were analyzed by SDS-PAGE and by immunoblotting for BRCA2, DSS1 and RAD51 with indicated antibodies.

(D) Homologous DNA pairing and strand exchange reactions with BRCA2 (10 or 20 nM) without or with DSS1 (15 nM or 30 nM with 10 nM BRCA2; 60 nM with 20 nM BRCA2) and RPA (90 nM). The mean values (± s.d.) of data from three independent experiments were plotted.

Figure S6 (sung)

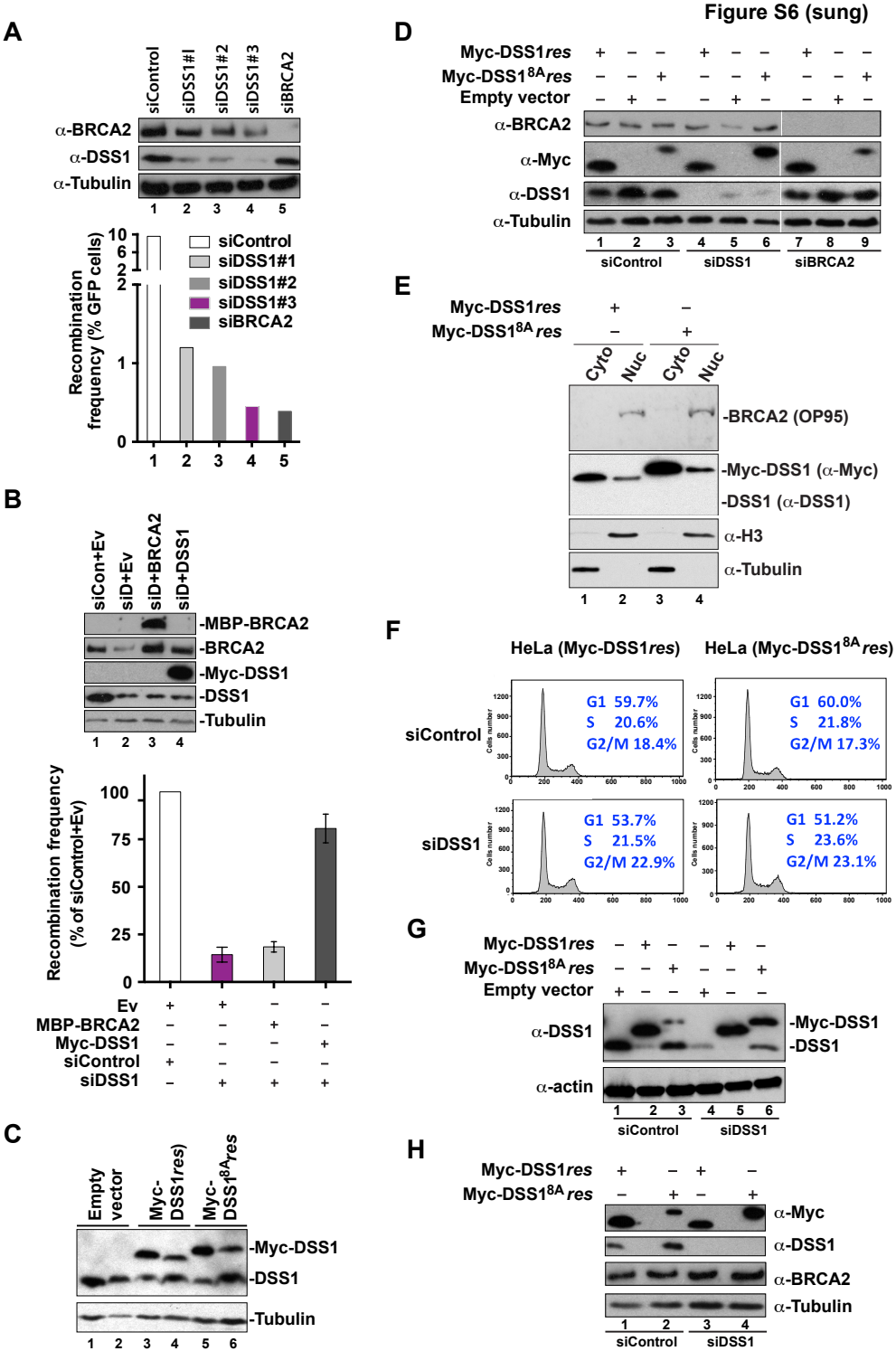

Figure S6 (sung)

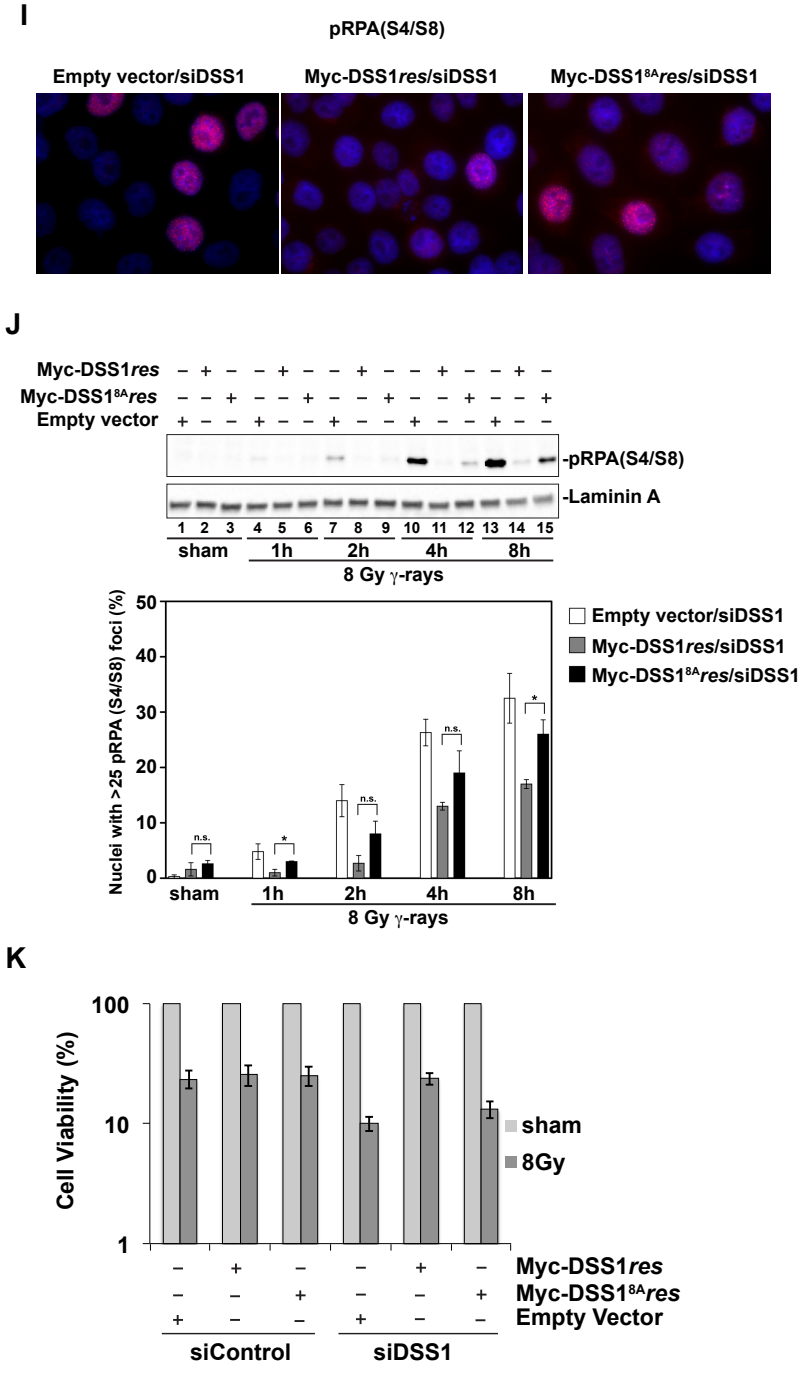

Figure S6. Genetic characterization of U2OS and HeLa cells stably expressing Myc-DSS1*res* or Myc-DSS1^{8A}*res*, related to Figure 6.

(A) Western blot analysis to detect endogenous DSS1 or BRCA2 after treatment of DR-U2OS cells with DSS1 or BRCA2 siRNA (top). HR efficiency in cells with siRNA-mediated knockdown of DSS1 or BRCA2 (bottom). Tubulin acts as the loading control.

(B) Western blot analysis to detect DSS1 or BRCA2 after the treatment of DSS1 siRNA and transient ectopic expression of MBP-BRCA2 and Myc-DSS1*res* in DR-U2OS cells (top). Examination of the relative HR levels in these cells (bottom). Ev: empty vector. Tubulin acts as the loading control.

(C) Levels of stably expressed Myc-DSS1*res* or Myc-DSS1^{8A}*res* and endogenous DSS1 in DR-U2OS cells. Two different stable cell lines with empty vector or expressing either Myc-DSS1*res* or Myc-DSS1^{8A}*res* used for the experiments in Figure 6B are shown.

(D) Western blot to examine the extent of protein depletion for the experiment in Figure 6B. Tubulin acts as the loading control.

(E) Western blot to examine the nuclear localization of endogenous BRCA2 and ectopic DSS1 in HeLa cells expressing Myc-DSS1*res* or Myc-DSS1^{8A}*res* and with endogenous DSS1 having been depleted by siRNA treatment. The cytoplasmic and nuclear fractions were analyzed for their alpha-Tubulin and histone H3 contents as well.

(F) Cell cycle analysis of samples used for the experiment in Figure 6E.

(G) Western blot to examine the extent of protein depletion for the experiment in Figure 6C & D. Actin was included as the loading control. The apparent lower amount of endogenous DSS1 in lane 2 and of Myc-DSS1^{8A}*res* in lane 3 might have stemmed from an uneven transfer of proteins to the PVDF membrane for immunoblotting.

(H) Western blot to examine the extent of protein depletion for the experiment in Figure 6E. Tubulin was included as the loading control.

(I) Representative micrographs of p-RPA(S4/S8) foci (red) in HeLa cell nuclei at 8 h after exposure to 8 Gy γ -rays. Blue: DAPI.

(J) Western blot to show pRPA(S4/S8) levels (upper panel; Laminin A as the loading control) and quantification of p-RPA(S4/S8) foci at various time points after exposure to 8 Gy γ -rays or sham irradiation (lower panel). The mean values ± s.e.m. of at least three independent experiments are shown. n.s., not significant and *, $P<0.05$.

(K) Cell viability of HeLa cell lines with empty vector or stably expressing Myc-DSS1*res* or Myc-DSS1^{8A}*res* after exposure to 8 Gy X-rays. The mean values (± s.d.) from three independent experiments were plotted. Data have been corrected for the plating efficiency of sham-irradiated cultures.

Figure S7 (sung)

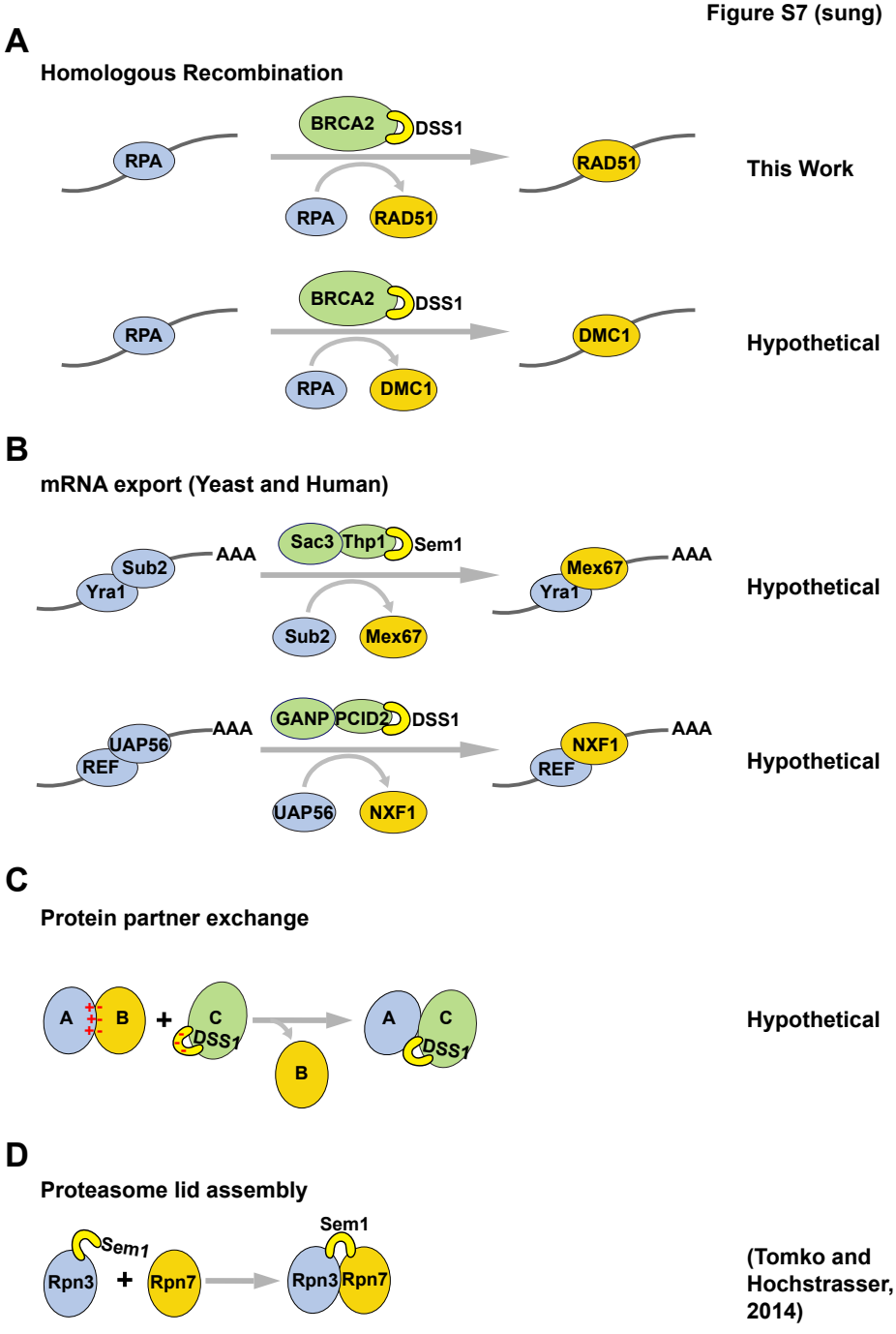

Figure S7. DSS1-mediated exchange of proteins on nucleic acids, related to Figure 7.

(A) Our results have revealed that DSS1 acts a DNA mimic in facilitating RPA-RAD51 exchange on ssDNA in homologous recombination (upper panel). We postulate that the BRCA2-DSS1 complex functions in a similar manner in the mediation of DMC1-ssDNA presynaptic filament assembly (lower panel).

(B) We postulate that, during mRNA export, Sem1 (the budding yeast ortholog of DSS1) and DSS1 function as a RNA mimic, to promote the exchange of Sub2 for Mex67 (upper panel) or UAP56 for NXF1 (lower panel).

(C) Model of DSS1 acting to mediate the exchange of protein partners to form a new protein complex.

(D) Role of Sem1 as a chaperone in facilitating proteasome lid assembly (Tomko and Hochstrasser, 2014)

Table S1 Oligonucleotides and siRNA used in this study.

Oligo 1	GACATCACCGGTCGCCACCGAGCAGAAGCTGATCTCAGAGGAGGACCTGTGATGGTGAG CAAGGGCGAGGAG
Oligo 2	CTCCTCGCCCTTGCTCACCATCACAGGTCCTCCTCTGAGATCAGCTTCTGCTCGGTGGCGA CCGGTGATGTC
Oligo 3	TGGGATGATGACAATGTAGAAGATGACTTTTCTAACCAGCTACGTGCTGAGCTGG
Oligo 4	CCAGCTCAGCACGTAGCTGGTTAGAAAAGTCATCTTCTACATTGTCATCATCCCA
Oligo 5	GAAGAGTTCCCTGCCGCAGCCGCGGCTGGCTTAGATGAAGAT
Oligo 6	ATCTTCATCTAAGCCAGCCGCGGCTGCGGCAGGGAACTCTTC
Oligo 7	CCGAAGACTGGGCTGGCTTAGCTGCAGCTGCAGCTGCACATGTCTGGGAGGATAATTG
Oligo 8	CAATTATCCTCCCAGACATGTGCAGCTGCAGCTGCAGCTAAGCCAGCCCAGTCTTCGG
Oligo 9	GAAGAGTTCCCTGCCGCAGCCGCGGCTGGCTTAGCTGCAGCTGCAGCTGCACATGTCTGG GAGG
Oligo 10	CCTCCCAGACATGTGCAGCTGCAGCTGCAGCTAAGCCAGCCGCGGCTGCGGCAGGGAAC TCTTC
Oligo 11	GTTCGAGGAGTTTCCCGCGGCAGCCGCGGCTGGCTTAGCTGCAGCTGCAGCTGCACATGT CTGGGAGGATAATTG
Oligo 12	CAATTATCCTCCCAGACATGTGCAGCTGCAGCTGCAGCTAAGCCAGCCGCGGCTGCCGCG GGAAACTCCTCGAAC
siControl	UAGCCGGUAGACUUAGGUCUG
siDSS1#1	UAGCCGGUAGACUUAGGUCUG
siDSS1#2	AAGAGUUCCCUGCCGAAGACU
siDSS1#3	UAGAGGAUGACUUCUCUAAUC
siBRCA2	UUGGAGGAAUAUCGUAGGUAA

Table S2. Intensities (signal strength) of RAD51 foci in control HeLa cells (empty vector) and HeLa cell derivatives (Myc-DSS1*res* and Myc-DSS1^{8A}*res*) after 8 Gy X-rays or sham irradiation, related to Figure 6.

	Empty vector /siControl	Empty vector /siDSS1	Myc-DSS1*res* /siControl	Myc-DSS1*res* /siDSS1	Myc-DSS1^{8A}*res* /siControl	Myc-DSS1^{8A}*res* /siDSS1
Sham	89.7	78.4	100.6	95.8	100.4	95.2
8Gy-2h	100.4	81.6	96.2	98.9	106.1	81.5
8Gy-4h	121.1	82.3	113.8	119.8	118.4	103
8Gy-8h	117.9	78.1	114.9	118.83	115.3	105.4
8Gy-24h	142.1	79.3	132.7	151	137.6	139.5

Extended Experimental Procedures

Plasmid construction

The cDNAs for full length BRCA2 and miBRCA2 (containing BRC repeat 4 (BRC4; residues 1496–1596), the DNA-binding domain (DBD; residues 2477–3194) and the C-terminal RAD51-binding domain (CTRB; residues 3195-3418)) were introduced into pDEST8 (Invitrogen) for bacmid production in *E. coli*. To facilitate protein purification, amino-terminal MBP and His_6 tags and a carboxyl-terminal Flag tag were engineered into BRCA2 and a C-terminal His_6 tag was attached to miBRCA2. The DSS1 cDNA was cloned into pDEST20 and pGEX4T-1 for the expression of GST-DSS1 in insect cells and *E. coli,* respectively. The mammalian Myc-DSS1 expression vector pMyc-DSS1*res* was generated from pEGFP-DSS1 (gift from Alan Ashworth). Quikchange site-directed mutagenesis was used to add a C-terminal Myc tag and to introduce silent mutations into the siRNA target regions using oligos 1 & 2 and oligos 3 & 4, respectively (see Table S1).

GST-tagged DSS1^{3A}, DSS1^{5A} and DSS1^{8A} and pMyc-DSS1^{8A}*res* were generated with oligos 5 & 6, 7 & 8, 9 & 10, 11 & 12, respectively, in the above protein expression vectors.

Protein purification

Purification of BRCA2 and miBRCA2 from insect cells

pDEST8-miBRCA2-His_6, pDEST8-MBP-His_6-BRCA2-Flag, and pDEST20-DSS1 were introduced into *E. coli* strain DH10Bac for bacmid generation. The bacmids were verified by PCR and used to transfect SF9 insect cells to generate recombinant baculoviruses. After amplification in SF9 cells, the viruses were used to infect Hi5 insect cells for expression of BRCA2 or miBRCA2 alone (10 ml viruses per 600 ml cells) or together with DSS1 (15 ml BRCA2 or miBRCA2 viruses and 7.5 ml DSS1 viruses per 600 ml cells). After a 44-h incubation at 27°C, cells were harvested by centrifugation, frozen in liquid nitrogen, and stored at -80°C. All the purification steps were carried out at 0°C to 4°C. To prepare extract, the frozen cell paste (8 g, from 600 ml culture) was thawed and suspended in 40 ml of cell breakage buffer A (50 mM Tris-HCl, pH 7.5, 300 mM KCl, 1 mM 2-mercaptoethanol, 0.05% Igepal CA-630, 5 mM $MgCl_2$, 2 mM ATP and the following protease inhibitors: aprotinin, chymostatin, leupeptin, and pepstatin A at 3 μg/ml each, and 1 mM PMSF).

For BRCA2 and BRCA2-DSS1, the final concentration of NP40 was adjusted to 0.5% for cell lysis using a homogenizer. The lysate was cleared by centrifugation at 10,000 × g for

15 min, and the supernant was incubated with 1 ml anti-Flag M2 affinity resin (Sigma) for 3 h. The beads were poured into a column (1.5 × 15 cm), washed with 30 ml lysis buffer and then 30 ml buffer B (25 mM Tris-HCl, pH 7.5, 300 mM KCl, 10% glycerol, 0.5 mM EDTA, 0.01% Igepal CA-630, 1 mM 2-mercaptoethanol, 5 mM $MgCl_2$ and 2 mM ATP). Proteins were eluted with 200 μg/ml Flag peptide in buffer B five times (1 ml each), which were pooled and mixed with 0.3 ml amylose resin for 1 h. The resin was washed with 10 ml buffer B and then treated with 10 mM maltose in buffer B five times (0.3 ml each) to elute proteins. These were pooled and incubated with 0.15 ml Glutathione Sepharose 4 Fast Flow resin (GE Healthcare) for 1 h. The resin was washed sequentially with 5 ml of buffer B containing 600 mM KCl and 10 ml buffer B, before being eluted five times with 0.15 ml of 20 mM glutathione in buffer B (this step was omitted in the purification of BRCA2). The protein pool from the amylose (for BRCA2) or glutathione (for BRCA2-DSS1) affinity step was loaded onto a Q Sepharose column (50 μl), which was washed with 5 ml buffer B before being eluted with buffer C (25 mM Tris-HCl, pH 7.5, 10% glycerol, 0.5 mM EDTA, 0.01% Igepal CA-630 and 1 mM 2-mercaptoethanol) containing 500 mM KCl five times (50 μl each). The peak fractions were pooled, frozen in liquid nitrogen, and stored at -80°C.

For miBRCA2 and miBRCA2-DSS1, the cells were lysed by sonication. After centrifugation (100,000 × g for 90 min), the clarified lysate was incubated with 5 ml Ni^{2+} NTA-agarose for 1 h. The matrix was poured into a column (1.5 × 15 cm), washed with 30 ml buffer B containing 600 mM KCl and then with 10 ml of 20 mM imidazole in buffer B, before being eluted with 10 ml each of 200 mM imidazole in buffer C 3 times.

The eluate was mixed with 1 ml Glutathione Sepharose 4 Fast Flow resin for 1 h, and the resin was washed and bound proteins were eluted as described above for BRCA2-DSS1 (this step was omitted for the purification of miBRCA2). The eluate was fractionated in a 2 ml heparin (Bio-Rad) column, using a 20 ml gradient of 150-1000 mM KCl in buffer C. The miBRCA2-DSS1 containing fractions (250-400 mM KCl) were combined and diluted with three volumes of buffer C before being further fractionated in a 1 ml Mono S column (Amersham Pharmacia Biotech), using a 15 ml gradient of 50-300 mM KCl in buffer C. The final pool of protein was concentrated in a Centricon-30K concentrator (Amicon), frozen in liquid nitrogen, and stored at -80°C. The miBRCA2-DSS1^{8A} complex was expressed and purified using the same procedures.

Purification of GST-DSS1, DSS1 and DSS1 mutants from *E. coli*

GST-DSS1 in pGEX4T-DSS1 were introduced into Rosetta (DE3) cells. Single colonies were expanded in 250 ml LB medium overnight at 37°C before dilution into 10 L fresh LB medium. Expression of GST-DSS1 was induced by the addition of 0.4 mM IPTG when the cell density had reached OD600 = 0.8, and cells were harvested after a 16-h incubation at 16°C. The pellet (20 g, from 5 L culture) was suspended in 100 ml buffer D (20 mM KH_2PO4, pH 7.5, 10% glycerol, 0.5 mM EDTA, 0.01% Igepal, 1 mM 2-mercaptoethanol and 300 mM KCl) containing the following protease inhibitors: aprotinin, chymostatin, leupeptin, and pepstatin A at 3 μg/ml each, and 1 mM PMSF, and lysate was prepared by sonication. After centrifugation (100,000 × g for 90 min), the clarified lysate was incubated with 5 ml Glutathione Sepharose 4 Fast Flow resin for 2 hours. The resin was poured into a column (1.5 x 15 cm), washed with 50 ml buffer

C, before being eluted 3 times with 10 ml of 10 mM glutathione in buffer E (20 mM KH_2PO4, pH 7.5, 10% glycerol, 0.5 mM EDTA, 0.01% Igepal, 1 mM 2-mercaptoethanol and 100 mM KCl). The eluate was loaded onto a Q Sepharose column (10 ml total), which was developed with a 120 ml gradient of 200-600 mM KCl in buffer C. Fractions containing GST-DSS1 (360-480 mM KCl) were pooled, concentrated in a Centricon-10K concentrator (Amicon), frozen in liquid nitrogen, and stored at -80°C. For removing the GST tag, purified GST-DSS1 (10 mg) was immobilized on Glutathione resin (1 ml), which was washed with 50 ml buffer D before being incubated with 50 units of thrombin (GE Healthcare Life Sciences) in 1 ml buffer D without the protease inhibitors at 4°C for 18 h. The supernatant that contained DSS1 was concentrated in a Centricon-3K concentrator (Amicon), frozen in liquid nitrogen, and stored at -80°C. GST-$DSS1^{3A}$, GST-$DSS1^{5A}$, GST-$DSS1^{8A}$ and $DSS1^{8A}$ were expressed and purified using the procedures developed for the wild type counterpart.

Other recombination proteins

RAD51 and RPA were expressed in *E. coli* and purified to near homogeneity using our previously described procedures (Sigurdsson et al., 2001). *E. coli* SSB was purchased from Promega.

Affinity pulldown

RAD51 (5 μM) or RPA (3 μM) was incubated with 3 μM of miBRCA2, miBRCA2-DSS1, miBRCA2-$DSS1^{8A}$, GST, GST-DSS1 or GST-$DSS1^{8A}$ at 4°C for 30 min in 30 μl buffer F (25 mM Tris-HCl pH 7.5, 10% Glycerol, 0.5 mM EDTA, 0.01% Igepal CA-630

(Sigma), 1 mM 2-mercaptoethanol, 150 mM KCl). After this incubation, the reaction mixtures were gently mixed at 4°C for 30 min with 12 μl Ni^{2+} NTA-agarose or Glutathione Sepharose 4 Fast Flow resin to immobilize protein complexes through the $(His)_6$ tag on miBRCA2 or the GST tag on DSS1, respectively. The resin was washed three times with 100 μl buffer F and then treated with 20 μl 2% SDS to elute the protein complexes. The supernatant (S), last wash (W) and SDS eluate (E), 8 μl each, were analyzed by SDS-PAGE. For the pulldown experiments with the RPA-ssDNA complex, 100 nM GST-DSS1 and RPA and 4.5 μM (nucleotides) of dT30 were used. For pulldown experiments with BRCA2, the same procedure was applied except that 20 nM BRCA2 and RPA were used in the reaction.

DNA binding assay

5' ^{32}P-labeled dT30 (0.9 μM nucleotides) were incubated at 37°C for 10 min either with a mixture of RPA and DSS1 or with RPA first for 5 min followed by the addition of DSS1 in 10 μl buffer G (25 mM Tris-HCl, pH 7.5, 50 mM KCl, 1 mM dithiothreitol, and 100 μg/ml bovine serum albumin) for 10 min. After the addition of gel loading buffer (50% glycerol, 20 mM Tris-HCl, pH 7.4, 0.5 mM EDTA, 0.05% orange G), the reaction mixtures were resolved by 8% native polyacrylamide gel electrophoresis in 1 × TBE buffer (90 mM Tris-borate, pH 8.3, 2 mM EDTA) at 4°C. The gels were dried, and the products were visualized by autoradiography and quantified using the Quantity One software in the Personal Molecular Imager™ (Bio-Rad).

Homologous DNA pairing assay

The reaction was assembled in buffer G that contained 1 mM ATP and 2 mM $MgCl_2$ in a final volume of 12.5 μl. Unless stated otherwise, the steps were carried out at 37°C. In the standard reaction, the 150-mer oligo 3 (6 μM nucleotides) was incubated with RAD51 (2 μM) with or without the indicated concentration of miBRCA2 for 5 min, followed by the addition of ^{32}P-labeled homologous dsDNA (6 μM base pairs) and 4 mM spermidine hydrochloride. After 30 min of incubation, the reactions were mixed with an equal volume of 1% SDS containing 1 mg/ml proteinase K. Following a 5-min incubation, the deoproteinized reaction mixtures were resolved in 10% non-denaturing polyacrylamide gels in TAE buffer (30 mM Tris-acetate, pH 7.4, 0.5 mM EDTA) at 4°C. The gels were dried and analyzed as above. For evaluating the recombination mediator function of miBRCA2, ssDNA was preincubated with RPA (600 nM) or SSB (4 μM) for 5 min. For experiments with BRCA2, the same procedure was followed except that 200 nM RAD51, 90 nM RPA or 400 nM SSB, 600 nM ssDNA, and 600 nM dsDNA were used.

Magnetic bead-based pulldown to assess RAD51 loading onto ssDNA

RAD51 (70 nM) was pre-incubated with or without the indicated amounts of miBRCA2, miBRCA2-DSS1 or miBRCA2-DSS1^{8A} in 15 μl of buffer G with 1 mM ATP and 2 mM $MgCl_2$ at 25°C for 10 min. Then, biotinylated dT_{83} (200 nM) with or without prebound RPA (25 nM) was added to the reaction, followed by a 10-min incubation at 37°C. An 8-μl aliquot of the reaction (30 μl) was removed, combined with 8 μl 2 × SDS-PAGE loading buffer, and set aside as the input fraction. The remaining portion of the reaction

was incubated with 3 μl Streptavidin magnetic beads (Roche Applied Science) for 10 min at 25°C, followed by capture of the beads using a Magnetic Particle Separator (Roche Applied Science). The beads were washed twice with 30 μl of buffer G containing 0.02% Igepal CA-630, 1 mM ATP and 2 mM $MgCl_2$ before treatment with 22 μl 1 × SDS-PAGE loading buffer to elute proteins from the DNA. The input and eluate (5 μl each) were analyzed by SDS-PAGE and immunoblotting using antibodies against RAD51, RPA70 and BRCA2 (see **Immunoblot analysis** section below) to determine their content of proteins.

Electron microscopy

The reaction mixtures were assembled with combinations of RAD51 (2 μM), RPA (600 nM), miBRCA2 or miBRCA2-DSS1 or miBRCA2-DSS18A (150 nM), and the 150-mer ssDNA (6 μM nucleotides), as described for the homologous DNA pairing assay, except that BSA was omitted from the reaction buffer. After a 10-min incubation, the reactions were processed and examined in a Tecnai 12 transmission electron microscope following our published procedure (San Filippo et al., 2006).

Isothermal titration calorimetry

The interaction of DSS1 with RPA70N or RPA70NAB was quantified by measuring the heat changes during addition of DSS1 to the RPA fragment using a MicroCal VP-isothermal titration calorimeter. Protein samples were exchanged into 20 mM Tris-HCl (pH 7.2), 100 mM NaCl and 2 mM 2-mercaptoethanol prior to the experiment. Titrations were performed by first injecting 2 μl of 1 mM DSS1 into 75 μM of RPA70N or

RPA70NAB in the sample cell, followed by additional 10 μl injections. Results were analyzed using Origin software (MicroCal). Binding constants (K_d) and thermodynamic parameters were calculated by fitting the data to the best binding model using a nonlinear least-squares fitting algorithm.

NMR spectroscopy

NMR experiments were performed on Bruker DRX 600-MHz or 800-MHz spectrometers equipped with cryoprobes. ^{15}N-^{1}H heteronuclear single-quantum coherence (HSQC) spectra were acquired using 1024 complex points in the ^{1}H dimension and 128 complex points in the ^{15}N dimension. All spectra were collected at 25ºC using ^{15}N-enriched RPA70N, RPA70AB, RPA70NAB or DSS1 at 100 μM in a buffer containing 20 mM Tris (pH 7.2), 75 mM NaCl and 2 mM DTT. Titrations were monitored by acquiring a series of ^{15}N-^{1}H HSQC spectra for ^{15}N-enriched samples over the course of addition of unlabelled binding partner(s). All spectra were processed by Topspin v2.0 (Bruker, Billerica, MA) and analyzed with Sparky (University of California, San Francisco, CA). Chemical shift perturbations were calculated using the formula $\Delta\delta j = [(\Delta\delta j^{15}N/5)^2 + (\Delta\delta j^{1}H)^2]^{1/2}$.

Immunoblot analysis

Protein was extracted from cells harvested two days after transfection using NETN buffer (20 mM Tris pH 8, 100 mM NaCl, 1 mM EDTA, 0.5% IGEPAL, 1 mM DTT, and Roche Protease Inhibitor Cocktail) and 8 freeze/thaw cycles. Blots were probed with the following antibodies for detection by ECL (Thermo Scientific Pierce): DSS1 (Santa Cruz

Biotech, sc-28848), BRCA2 (EMD Millipore, OP95-100UG), RAD51 (Santa Cruz Biotech, sc-8349), RPA70 (Abcam ab79398), pRPA(S4/S8) (Bethyl Laboratories, A300-245), Actin (Abcam, ab3280), Myc.A7 (Abcam ab18185), Histone H3 (ab1791), Tubulin (Santa Cruz Biotech, sc-53030), Laminin A (Abcam, ab26300), HA.11 (16B12) (Covance, MMS-101P), MBP-HRP (NEB, E8038S), GST-HRP (NEB, E2624S) and HRP-conjugated secondary antibodies (Pierce 31450 for anti-mouse IgG-HRP in Rabbit, Sigma A6154 for anti-Rabbit IgG-HRP in Goat and Santa Cruz Biotech Sc-2032 for anti-Rat IgG-HRP in Goat).

Measurement of HR frequency by DR-GFP assay

The DR-U2OS cell line contains a single integrated copy of DR-GFP reporter. For HR assays, 2×10^5 exponentially growing cells per well were seeded in 6-well plates prior to transfection with 2 μl siRNA (20 μM) using 3 μl Lipofectamine™ 2000 (Invitrogen). One day after siRNA transfection, these cells were transfected with 2 μg I-*Sce*I expression vector (pCBASce) using 5 μl Lipofectamine 2000. Then, HR was measured by counting the fraction of GFP-positive cells using a BD FACS Calibur S at 72 h after I-*Sce*I transfection. The results were derived from 3 to 5 transfections of at least 3 independent experiments, and p-values were calculated using an unpaired *t*-test through Graphpad software (http://www.graphpad.com/quickcalcs/ttest1.cfm).

Immunofluorescence microscopy and image analyses

Cells in exponential growth were transfected on two consecutive days in Opti-MEM medium using RNAiMAX (Invitrogen) with 20 nM DSS1 or control siRNA, as

recommended by the manufacturer. X-ray exposures were carried out on the next day using a 6.3 mA 160 kVp X-ray machine at a dose rate of 1.8 Gy/min. Exposure to γ-ray was performend using a ^{137}Cs γ-irradiator (J.L. Shepherd, model 81-14) using a dose rate of 1.05 Gy/min. Immunohistochemistry was performed as previously (Wiese et al., 2007), except that cells were fixed in 4% paraformaldehyde at room temperature for 10 min and premeabilized in 0.5% Triton X-100 in PBS for 5 min. Rabbit anti-RAD51 (H-92; Santa Cruz Biotechnology; 1:500) and anti-pRPA(S4/S8) (A300-245; Bethyl Laboratories) antibodies and AlexaFluor-488 or -594 goat anti-rabbit IgG (Invitrogen; 1:500) were used. For image capture of RAD51 foci, 10 Z-stack section images (0.7 μm intervals) were taken per sample using a confocal Zeiss LSM-710 laser scanning microscope with 100× magnification and Zeiss Zen 2011 software (version 7.1). For image capture of pRPA(S4/S8) foci, 10 Z-stack section images were taken per sample each consisting of 24 stacks (0.3 μm intervals) using a 63× oil objective and a Zeiss Axio-Imager.Z2 microscope equipped with Metamorph software (Molecular Devices, Sunnyvale, CA).

For computational analyses of RAD51 foci, Z-stacks were collapsed down to the maximum intensity projections. All images were registered with the BioSig (Biological Signature) Imaging Bioinformatics Platform, as described (Parvin et al., 2007). Image analysis included nuclear segmentation using convexity (Raman et al., 2007). For computational analyses of pRPA(S4/S8) foci, Z-stacks were collapsed down to the maximum intensity projections and a combination of ImageJ (http://rsb.info.nih.gov/ij/) and Cell Profiler (http://www.cellprofiler.org/) software programs was used with the

following custom program settings for image processing: minimum object size = 3; maximum object size = 35; despeckle ratio = 0.3; rolling ball size = 5. A custom-built pipeline for automated cell (80 – 300 pixel units) and pRPA(S4/S8) foci counting with settings for shape (i.e. 0.5) and dimensions (i.e. 5 pixels diameter) was employed. Foci detected were first normalized to their respective control samples (sham irradiated) and counted as positive nuclei only,if they had > 25 foci/nucleus. Statistical significance was assessed by two-tailed unpaired Student's t-test. $P \leq 0.05$ was considered significant.

Clonogenic survival and cell viability assays

Hela cells were transiently transfected with siRNA as described above. After 48 hours, cells were seeded into 6-well plates at 50-32,000 cells/well, treated with 0, 5, 10 and 20 ng/ml MMC (Sigma) or 0, 0.5, 2 and 4 μM Olaparib (Selleckchem) in regular growth medium for 14 days. Cells were fixed with 10% methanol and 10% acetic acid, and stained with 1% crystal violet in methanol before colonies were counted. Clonogenic survival was determined for a given concentration of cells that were plated by dividing the number of colonies on each treated plate by the number of colonies on each untreated plate taking the plating efficiency of untreated cells into account. To determine cell viability, HeLa cells were seeded in 6-well plates at 25,000 cells/well after 8 Gy X-rays. After 4 days in culture, cells were fixed and stained as above for the clonogenic survival assay. The plates were rinsed in water to remove excess crystal violet, and the dye was dissolved with methanol/0.1% SDS solution to determine the OD at 595 nM. For quantitation, the OD595 value of each well was normalized to the respective value of

untreated cells corrected for their plating efficiency and corrected for background staining obtained from a well without any cells seeded.

Preparation of cytoplasmic and nuclear extracts

The Dignam method for the preparation of cytoplasmic and nuclear extracts (Dignam et al., 1983) was followed. Briefly, 10^9 cells were washed with PBS and Dignam buffer A (10 mM Hepes pH 7.9, 1.5 mM $MgCl_2$, 10 mM KCl, 0.5 mM DTT and 0.5 mM PMSF), collected by centrifugation, and lyzed in 2 packed cell volumes of Dignam buffer A using a Dounce homogenizer with the type A pestle. After centrifugation, the supernatant containing cytoplasmic proteins was saved for analysis. The pelleted nuclei were resuspended and lysed in 3 ml Dignam buffer C (20 mM Hepes pH 7.9, 1.5 mM $MgCl_2$, 420 mM NaCl, 0.2 mM EDTA, 0.5 mM DTT, 25% glycerol, and 0.5 mM PMSF) using a Dounce homogenizer with the type B pestle. Debris was removed by centrifugation to yield the nuclear extract fraction.

Analysis of cell cycle profile

For this analysis, 10^6 cells were washed with cold PBS, collected by centrifugation, and then fixed in 10 ml of ice-cold 70% ethanol/PBS for at least 2 days at 4ºC. The fixed cells were washed sequentially with 1 ml each of 30% ethanol/PBS and 0.05% BSA/PBS at 4ºC. Cells were incubated in the staining solution (40 μg/ml RNase A and 30 μg/ml propidium iodide in PBS) for 15 min at 37°C in the dark. The stained cells were fractionated in a BD FACS Calibur S instrument and analyzed by the FlowJo software.

Supplemental References

Dignam JD, Lebovitz RM, Roeder RG (1983). Accurate transcription initiation by RNA polymerase II in a soluble extract from isolated mammalian nuclei. Nucleic Acids Res *11*, 1475-1489.

Parvin, B., Yang, Q., Han, J., Chang, H., Rydberg, B., and Barcellos-Hoff, M.H. (2007). Iterative voting for inference of structural saliency and characterization of subcellular events. IEEE Trans Image Process *16*, 615-623.

Raman, S., Maxwell, C.A., Barcellos-Hoff, M.H., and Parvin, B. (2007). Geometric approach to segmentation and protein localization in cell culture assays. J Microsc *225*, 22-30.

San Filippo, J., Chi, P., Sehorn, M.G., Etchin, J., Krejci, L., and Sung, P. (2006). Recombination mediator and Rad51 targeting activities of a human BRCA2 polypeptide. J Biol Chem *281*, 11649-11657.

Sigurdsson, S., Trujillo, K., Song, B., Stratton, S., and Sung, P. (2001). Basis for avid homologous DNA strand exchange by human Rad51 and RPA. J Biol Chem *276*, 8798-8806.

Tomko, R.J., Jr., and Hochstrasser, M. (2014). The Intrinsically Disordered Sem1 Protein Functions as a Molecular Tether during Proteasome Lid Biogenesis. Mol Cell *53*, 433-443.

Wiese, C., Dray, E., Groesser, T., San Filippo, J., Shi, I., Collins, D.W., Tsai, M.S., Williams, G.J., Rydberg, B., Sung, P., *et al*. (2007). Promotion of homologous recombination and genomic stability by RAD51AP1 via RAD51 recombinase enhancement. Mol Cell *28*, 482-490.